

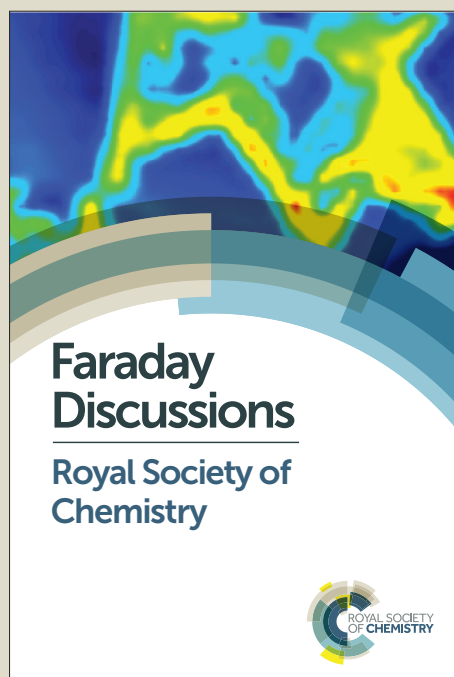
Faraday Discussions

Accepted Manuscript



This manuscript will be presented and discussed at a forthcoming Faraday Discussion meeting. All delegates can contribute to the discussion which will be included in the final volume.

Register now to attend! Full details of all upcoming meetings: <http://rsc.li/fd-upcoming-meetings>



This is an *Accepted Manuscript*, which has been through the Royal Society of Chemistry peer review process and has been accepted for publication.

Accepted Manuscripts are published online shortly after acceptance, before technical editing, formatting and proof reading. Using this free service, authors can make their results available to the community, in citable form, before we publish the edited article. We will replace this *Accepted Manuscript* with the edited and formatted *Advance Article* as soon as it is available.

You can find more information about *Accepted Manuscripts* in the [Information for Authors](#).

Please note that technical editing may introduce minor changes to the text and/or graphics, which may alter content. The journal's standard [Terms & Conditions](#) and the [Ethical guidelines](#) still apply. In no event shall the Royal Society of Chemistry be held responsible for any errors or omissions in this *Accepted Manuscript* or any consequences arising from the use of any information it contains.

This article can be cited before page numbers have been issued, to do this please use: C. Giorio, S. J. Campbell, M. Bruschi, A. T. Archibald and M. Kalberer, *Faraday Discuss.*, 2017, DOI: 10.1039/C7FD00025A.

Detection and identification of Criegee intermediates from the ozonolysis of biogenic and anthropogenic VOCs: comparison between experimental measurements and theoretical calculations

Chiara Giorio^{1a*}, Steven J. Campbell¹, Maurizio Bruschi², Alexander T. Archibald^{1,3}, Markus Kalberer^{1*}

¹ Department of Chemistry, University of Cambridge, Lensfield Road, Cambridge, CB2 1EW, United Kingdom

² Dipartimento di Scienze dell'Ambiente e del Territorio e di Scienze della Terra, Università degli Studi di Milano Bicocca, Piazza della Scienza 1, Milano, 20126, Italy

³ National Centre for Atmospheric Science, UK.

^a now at: Aix-Marseille Université, CNRS, LCE UMR 7376, 13331 Marseille, France

*correspondence to: chiara.giorio@atm.ch.cam.ac.uk; markus.kalberer@atm.ch.cam.ac.uk

Abstract

Ozonolysis of alkenes is a key reaction in the atmosphere, playing an important role in determining the oxidising capacity of the atmosphere and acting as a source of compounds that can contribute to local photochemical “smog”. The reaction products of the initial step of alkene-ozonolysis are Criegee intermediates (CIs), which have for many decades eluded direct experimental detection because of their very short lifetime. We use an innovative experimental technique, stabilisation of CIs with spin traps and analysis with proton transfer reaction mass spectrometry, to measure the gas phase concentration of a series of CIs formed from ozonolysis of a range of both biogenic and anthropogenic alkenes in flow tube experiments. Density functional theory (DFT) calculations were used to assess the stability of the CI-spin trap adducts and showed that the reaction of the investigated CIs with the spin trap occurs very rapidly except for the large β -pinene CI. Our measurement method was used successfully to measure all the expected CIs, emphasising that this new technique is applicable to a wide range of CIs with different molecular structures previously unidentified experimentally. In addition, for the first time it was possible to study CIs simultaneously in an even more complex reaction system consisting of more than one olefinic precursor. Comparison between our new experimental measurements, calculations of stability of the CI-spin trap adducts and results from numerical modelling, using the master chemical mechanism (MCM), showed that our new method can be used for quantification of CIs produced *in situ* in laboratory experiments.

Keywords

Criegee intermediates, VOC, PTR-MS, spin traps, MCM, DFT

1. Introduction

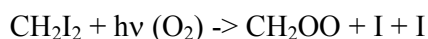
The Anthropocene has seen huge changes in the composition of the atmosphere. Gaseous, volatile organic compounds (VOCs) play an important role in determining the overall composition and reactivity of the atmosphere. Many VOC sources significantly changed since the onset of the Anthropocene in strength but new sources and VOCs have also emerged. Oxidative degradation in the atmosphere with oxidants such as ozone is one of the main removal process for VOCs. Olefinic VOCs react strongly with ozone leading to a complex reaction scheme with a large number of stable but also reactive intermediate reaction products. The initial step of alkene-ozone reactions is a 1,3-cyclo addition to produce a molozonide, which subsequently decomposes to produce so-called Criegee Intermediates (CI) and a carbonyl product. In the condensed phase a further rearrangement is possible, but this is not the case in the gas phase.¹⁻³





The formation of CIs was postulated over 40 years ago⁴ to proceed through the reaction of an alkene functional group with ozone (O₃) but only in the last decade has our understanding of the short-lived CIs begun to flourish. The CI that is produced is thermally “hot” (sometimes referred to as an excited CI) and may undergo spontaneous decomposition to form other products⁵ or collisions with other molecules to lead to the stabilised CI (SCI).

The majority of recent studies that directly detected and studied SCI in the gas phase used a different route to its formation than the ozonolysis mechanism described above (e.g. Welz et al.,⁶ and references therein). Rather than reaction between O₃ and unsaturated compounds, gem-iodo compounds have been shown to form CIs when photolysed in the presence of air:



The formation of SCIs *via* this reaction has enabled new studies to probe the kinetics of bimolecular reactions that the SCIs can undergo in the atmosphere. These studies have made use of a range of advanced laboratory techniques including photoionisation mass spectrometry and tunable synchrotron photoionisation mass spectrometry.^{6,7} Those techniques have been applied to the direct measurement of formaldehyde oxide, the simplest CI, and later on made possible the discovery of conformer-dependent reactivity of the *syn*- and *anti*-acetaldehyde oxides⁸, as these techniques are capable of distinguishing the two conformers from the difference in photoionisation energy. Subsequent studies detected formaldehyde oxide using near-UV cavity ring down spectroscopy⁹, UV-Vis spectroscopy^{10–12} and IR spectroscopy¹³. The latter was used also for direct detection of the large β-pinene Criegee from ozonolysis reaction.¹⁴

On the other hand, indirect measurements, exploiting the oxidation of SO₂ to H₂SO₄ in the presence of an ·OH scavenger, were used in Hyytiälä (a boreal forest in Finland) to quantify an oxidant “X” tentatively associated with SCIs with concentrations in the order of 5 × 10⁴ molecules cm⁻³.^{15,16} Other indirect methods exploited more specific reactions of organic reagents with CIs to identify their structure: Horie et al.¹⁷, who found that hexafluoro acetone reacts rapidly with CIs to form compounds which are assignable to ozonides, 3,3-di(trifluoro)methyl-1,2,4-trioxolanes, which can be detected in FTIR spectroscopy. Very recently we presented a new cost-effective method to stabilise and detect CIs online in the gas phase by reacting them with spin traps and analysing the adducts that form with proton transfer reaction time of flight mass spectrometry (PTR-ToF-MS)¹⁸. This method was successfully applied for the measurement of CIs from the ozonolysis of α-pinene, the structure of the CI-spin trap adduct was characterised in detail and we showed the potential of this technique to be used for quantification purposes.¹⁸

Here we expand on our previous study¹⁸ by measuring CIs from the ozonolysis of a series of biogenic and anthropogenic VOCs such as β-pinene, limonene, methacrolein, cis-2-hexene, styrene and also a mixture of more than one olefinic precursor. Experimentally measured concentrations of CI-spin trap adducts are compared with those which are theoretically expected, and differences explained in terms of stability of the CI-spin trap adducts and instrumental response. We demonstrate that our new technique is uniquely capable of quantifying many different CIs simultaneously and thus provides a significant step towards studying CIs in realistic, complex reaction mixtures.

2. Materials and methods

2.1. Chemicals

For the gas phase ozonolysis experiments, the following VOC precursors were used: styrene (≥99.9%, Reagentplus®, Sigma-Aldrich), R-(+)-limonene (≥99.0%, Sigma-Aldrich), methacrolein



($\geq 95\%$, Aldrich), (-)- β -pinene ($\geq 99.0\%$, Aldrich) and cis-2-hexene ($\geq 95\%$, Aldrich). The spin trap 5,5-dimethyl-pyrroline N-oxide (DMPO) ($\geq 97\%$, GC grade, Sigma-Aldrich) was used to capture and stabilise CIs in the gas phase.

2.2. Flow tube set-up

The experimental technique of using the spin trap DMPO to capture gas phase CIs with subsequent analysis of the adduct formed with PTR-ToF-MS has been described previously in detail.¹⁸ The ozonolysis reaction takes place in a flow tube reaction vessel, which is maintained at ambient temperature (~ 16 - 18°C) and pressure, and dry conditions (relative humidity $< 2\%$) as shown in Figure 1. The experimental set-up comprises of a 2.5 L glass flow tube, in which the olefinic precursor reacts with ozone with a reaction time of three seconds (see Figure S1 in Electronic Supplementary Information) before the sample flow is mixed with a N_2 flow containing the gaseous spin trap which scavenges and forms stable adducts with the CIs. A heated PTFE tube in which the spin trap reacts with the CI connects the mixing point with the PTR-ToF-MS for quantification. The olefinic precursors were evaporated from a 25 mL pear-shaped flask filled with 0.5 mL of pure compound and introduced continuously in the flow tube using N_2 (at $175\text{ cm}^3\text{ min}^{-1}$, oxygen-free nitrogen, BOC) carrier gas regulated *via* a 20 - $2000\text{ cm}^3\text{ min}^{-1}$ mass flow controller (MKS 1179A Mass-Flo® controller). For experiments with cis-2-hexene and methacrolein, due to the fact that they are more volatile compared to the other VOC precursors, the pear shaped flask was submersed in a dry ice/acetonitrile bath (-41°C) in order to maintain a lower steady-state concentration of these compounds in the flow tube. The other VOCs were maintained at ambient temperature. Ozone was produced by flowing synthetic air (Zero grade, BOC) past a UV lamp (185/254 nm, Appleton Woods®) at $155\text{ cm}^3\text{ min}^{-1}$ (20 - $2000\text{ cm}^3\text{ min}^{-1}$ MKS 1179A Mass-Flo® controller). The UV lamp used in this study produced a lower amount of ozone compared with the previous study on α -pinene ozonolysis,¹⁸ reaching a maximum concentration in our system of 18 ppm measured using a UV photometric ozone analyser (Thermo Scientific model 49i) and shown in Figure S2. The outlet of the flow tube is mixed into a T-connection (stainless-steel 1/4" ($\sim 6.35\text{ mm}$) T-fitting, Swagelok®) with a $310\text{ cm}^3\text{ min}^{-1}$ flow (50 - $5000\text{ cm}^3\text{ min}^{-1}$ MKS 1179A Mass-Flo® controller) of DMPO in N_2 (oxygen-free nitrogen, BOC) evaporated from a 25 mL flask filled with 0.5 mL of DMPO, which is held in a water bath at 40°C . Connecting tubes and the T-connection were kept at 85°C to avoid condensation of DMPO.

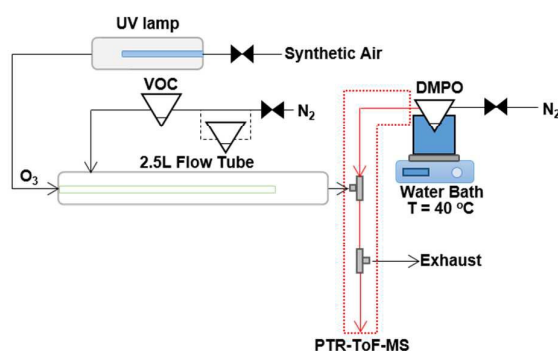


Figure 1. Schematic of the experimental set up, consisting of; a 2.5 L glass flow tube where an olefinic precursor reacts with ozone, a mixing point (T-fitting) in which the spin trap is mixed with the sample flow from the flow tube, and a heated PTFE tube in which the spin trap reacts with the CI before detection and quantification with PTR-ToF-MS. For the experiments where two VOC precursors were mixed, an additional pear shaped flask was added in-line with the N_2 carrier gas flow. Modified from Giorio et al.¹⁸



2.3. PTR-ToF-MS measurements

Online gas phase concentrations of the VOC precursors, DMPO and CI-DMPO adducts were measured using a proton transfer reaction time-of-flight mass spectrometer (PTR-ToF-MS 8000, Ionicon Analytik, Innsbruck, Austria) in the m/z range 10-500, with a time resolution of 10 s and a mass resolution $m/\Delta m$ of approximately 5000 (full width at half maximum) at the mass of protonated acetone. Source settings for all experiments were: drift tube pressure ~ 2.22 mbar, a drift tube voltage of 510 V and a drift tube temperature = 90°C; resulting in an E/N of ~ 127 Td (1 Td = 10^{-17} V cm²). The PTR-ToF-MS inlet (1 m long inert peek tube ID=1 mm, OD=1.59 mm) was kept at 100°C and the sampling flow rate was 100 cm³/min. Data analysis was conducted using PTR-MS Viewer 3.2 (Ionicon Analytik). The concentration of the olefinic precursors were estimated on the basis of the rate constant of the proton transfer reaction, which were: styrene (2.33×10^{-9} cm³ molecule⁻¹ s⁻¹), limonene (2.54×10^{-9} cm³ molecule⁻¹ s⁻¹), methacrolein (3.55×10^{-9} cm³ molecule⁻¹ s⁻¹) and β -pinene (2.50×10^{-9} cm³ molecule⁻¹ s⁻¹).¹⁹ The value for cis-2-hexene is unknown, so it was approximated to be the value for the isomer trans-2-hexene (2.05×10^{-9} cm³ molecule⁻¹ s⁻¹).¹⁹ For DMPO and the CI-DMPO adducts, ion-polar molecule capture collisions rate constant were calculated as detailed in Section S4 and elsewhere.^{20,21}

For quantification of the initial concentrations of β -pinene and limonene both the protonated molecular ion $C_{10}H_{17}^+$ and the fragment $C_6H_9^+$ were used, for cis-2-hexene both the protonated molecular ion $C_6H_{13}^+$ and the main fragment $C_3H_7^+$, for methacrolein the protonated molecular ion $C_4H_7O^+$ and the fragments $C_3H_7^+$ and $C_3H_5^+$ while for styrene only the protonated molecular ion $C_8H_9^+$ was used for quantification.

DMPO and VOC signals are often in saturation during the experiments and therefore the corresponding ¹³C isotopes were used for quantification. Initial concentration of VOCs and DMPO was also evaluated by diluting the sample flow with pure N₂ in a ratio 1:10 as detailed in Giorio et al.¹⁸

2.4. DFT calculations

Geometry optimizations and energy calculations have been carried out in the density functional theory (DFT) framework with the TURBOMOLE 6.4 suite of programs²² by using the BP86^{23,24} and B3LYP²⁵⁻²⁷ functionals, and a valence triple- ζ basis set with polarization functions on all atoms (TZVP).²⁸ For the BP86 functional the resolution-of-the-identity (RI) technique is applied.²⁹ As the geometries and the energy differences calculated by the two functionals are qualitatively similar and give the same interpretation of the results in the section 3.2 only B3LYP calculations will be discussed (see Figure 3 and Table S1 for the comparison of the BP86 and B3LYP results). Stationary points of the energy hypersurface have been located by means of energy gradient techniques and full vibrational analysis has been carried out to further characterise each stationary point and for the calculation of the thermochemical corrections for determining enthalpies at 298 K. The optimization of transition state structures has been carried out according to a procedure based on a pseudo Newton-Raphson method. The search of the transition state structure is carried out using an eigenvector-following algorithm in which, the search is performed by choosing the critical eigenvector with a maximum overlap criterion, which is based on the dot product with the eigenvector followed at the previous step. Finally, the analytical Hessian matrix is calculated to carry out the vibrational analysis of the stationary point. Energies of the van der Waals complexes have been corrected for the basis set superposition error using the procedure of Boys and Bernardi.³⁰ Average static polarisabilities have been calculated at the B3LYP/def-TZVP level of theory by using the first-order response theory as implemented in TURBOMOLE 6.4.^{31,32}

2.5. MCM modelling

We compare our experimental results with modelled time evolutions of SCIs using the AtChem (<https://atchem.leeds.ac.uk/>) numerical box-model. AtChem is developed for use with the Master Chemical Mechanism (MCM)³³. Model input parameters used in all simulations are included in



Table 1. In total, we performed six simulations using initial conditions from Table 1 and the mixing ratios of O₃ and the VOCs as measured in our flow tube experiments. AtChem was run on-line, making use of the most recent version (v1.5). The numerical model makes use of the Fortran CVODE library for the integration of the stiff ODEs that are represented by the MCM reaction mechanism. For each AtChem simulation we downloaded a unique MCM input file. This input file contained all the relevant inorganic and organic chemical reactions that were integrated forward in time by AtChem.

Table 1. Parameters and their values used in the AtChem box-model simulations of our flow tube experiments.

Parameter	Value (units)
Temperature	289.15 K
Number Density (M)	2.60x10 ¹⁹ (molecules cm ⁻³)
[H ₂ O]	1.23x10 ¹⁴ (molecules cm ⁻³)
[O ₃]	4.41x10 ¹⁴ (molecules cm ⁻³)

3. Results and discussion

We used stabilisation with the spin trap DMPO and analysis with PTR-ToF-MS to quantify the CIs produced from the ozonolysis of five VOCs (Figure 2). The VOCs under study have been chosen as representative of different classes of compounds of interest in atmospheric chemistry, including biogenic VOCs, such as β-pinene, limonene, methacrolein, and anthropogenic VOCs, such as cis-2-hexene and styrene. Among these, methacrolein also represents oxidised VOCs and styrene represents aromatic-olefins. The objective of this study is to assess the quantification capability of our new measurement technique. To do so, we used theoretical calculations to investigate the mechanism of formation of the CI-DMPO adducts, the energy barriers of these reactions and assess the stability of the adducts. Subsequently, we performed experiments of ozonolysis of the VOCs in a flow tube to detect and quantify the CI-DMPO adducts from the five individual VOCs and from a mixture of two different VOCs (namely β-pinene and cis-2-hexene). Additionally, we compared the experimentally measured concentrations of CI-DMPO adducts with those expected from numerical modelling, using the AtChem/MCM model.

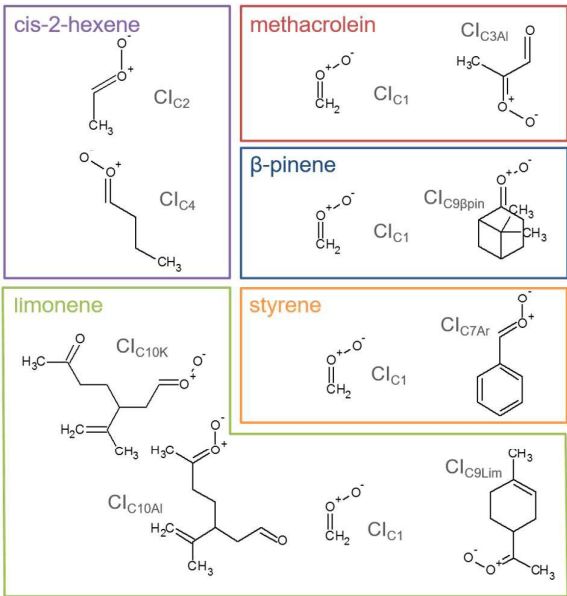


Figure 2. Molecular structures and acronyms of the CIs detected from the ozonolysis of cis-2-hexene, methacrolein, β-pinene, styrene and limonene.

3.1. Mechanism of formation and stability of CI-DMPO adducts

The measurement method used in this study, presented for the first time in Giorio et al.,¹⁸ is based on the stabilisation of the highly reactive CIs using the spin trap DMPO. Assessing the quantification capability can be challenging as the kinetics of formation of the CI-DMPO adducts and the stability of such adducts are unknown. To support and aid interpretation of our experimental results, the stability of the CI-DMPO adducts generated by the ozonolysis of β -pinene, cis-2-hexene and methacrolein, and the mechanism and energy barriers of their formation have been investigated by DFT calculations (see Figure 2 for the CIs).

An extensive search on the potential energy surface (PES) of these CIs was carried out to identify the relevant minimum energy conformations. It turns out that for CI_{C_2} , CI_{C_4} and $\text{CI}_{\text{C}_3\text{Al}}$ the *syn* conformation is more stable than the *anti* one by 1.8, 1.5 and 5.8 kcal/mol, respectively, whereas in $\text{CI}_{\text{C}_9\beta\text{pin}}$ the *anti* conformer is more stable than the *syn* conformer by about 2 kcal/mol (n.b. hereafter we will refer to the *syn* conformation as that in which the outer oxygen points toward the alkyl group in CI_{C_2} , CI_{C_4} and $\text{CI}_{\text{C}_3\text{Al}}$, and toward the less H-rich $\text{C}(\text{CH}_3)_2$ group in $\text{CI}_{\text{C}_9\beta\text{pin}}$; see Figure 3 for the definition of *syn* and *anti* conformations). It is worth noting that these results are in good agreement with previous calculations carried out using ab initio highly correlated methods.^{34–37} The addition of CIs with DMPO have been investigated by taking into account both *anti* and *syn* conformers to inspect potential differences in the reactivity of the two species.

The cycloaddition of the CIs to the spin-trap DMPO can occur through the attack of the carbon atom of the CI to either the nitrogen or the oxygen atoms of the DMPO nitron group leading to the formation of a 5-membered or a 6-membered ring respectively. DFT calculations show that for all of the compounds investigated the 6-membered ring species is much more stable than the corresponding 5-membered ring species (see Table S1), in agreement with the results obtained from the investigation of the formation of CI-DMPO adducts from the ozonolysis of α -pinene.¹⁸ Therefore, in the following only the addition of CIs to DMPO to give 6-membered ring adducts will be considered.



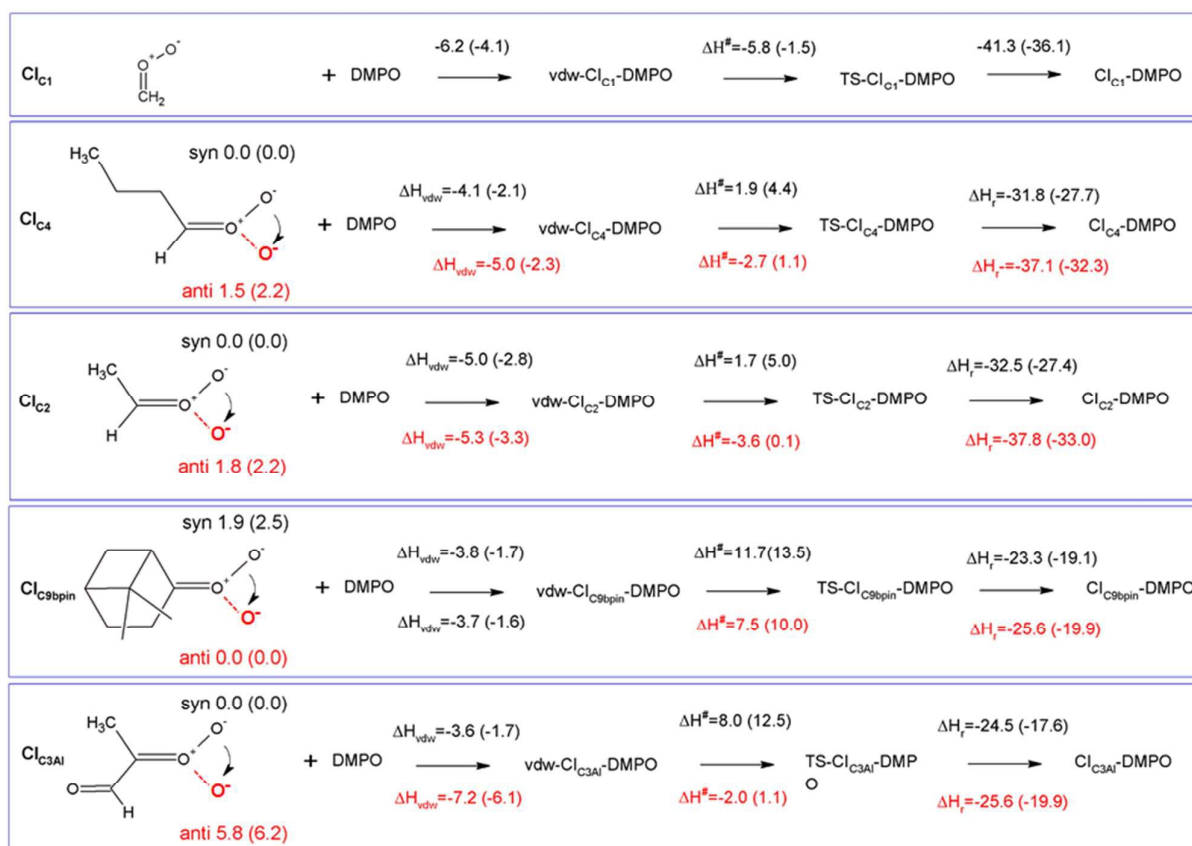


Figure 3. Schematic representation of the reaction of CIs with DMPO with values of reaction and activation enthalpies. The first step for each reaction is the formation of the van der Waals adduct (vdw-CI-DMPO), the second step is the formation of the transition state (TS-CI-DMPO) and the last step is the conversion to the final adduct (CI-DMPO). All values refer to enthalpy differences calculated with respect to the separated reactants using the B3LYP functional. In parenthesis are the corresponding values calculated using the BP86 functional. The molecular structures define the *anti* (black terminal oxygen) and the *syn* (red terminal oxygen) conformers. The values over (in black) and under (in red) the arrows refer to the reaction of the *anti* and *syn* conformers, respectively.

The first step in the reaction of the CIs with DMPO is the formation of pre-reactive van der Waals adducts in which the carbonyl oxide approaches the nitron group of DMPO (see Figures S9-S13). The interaction energies of such van der Waals complexes are within -3.6 and -7.2 kcal/mol, with the two extremes given by Cl_{C3Al} in the *syn* and *anti* conformations (see Figure 3).

The reactivity of the CIs strongly depends on the number of the substituents attached to the carbon atom of the carbonyl oxide, and on the initial conformation of the CI reactants (see Figures 5 and 6). The reaction of the parent formaldehyde oxide Cl_{C1} with DMPO is barrierless as the activation enthalpy is lower than the enthalpy of the separated reactants (ΔH[‡] = -5.8 kcal/mol), and only 0.5 kcal/mol higher than that of the van der Waals adduct. This reaction is also strongly exothermic with the value of the reaction enthalpy (ΔH_r) as low as -41 kcal/mol. The energy barriers for the addition to DMPO of Cl_{C2} and Cl_{C4}, featuring one alkyl substituent bounded to the carbon atom of the carbonyl oxide, are slightly larger than that calculated for the parent Cl_{C1}, and the reactions are slightly less exothermic. Indeed, when considering as reactants the most stable *syn* conformers (Cl_{C2(syn)} and Cl_{C4(syn)}) the energy barriers for both species are about 2 kcal/mol with respect to the separated reactants, and about 7 kcal/mol with respect to the van der Waals complexes. The reaction enthalpies of these two cycloadditions (ΔH_r) are also very similar and equals to about -32 kcal/mol. The reaction is still more favoured when starting from the less stable *anti* conformers (Cl_{C2(anti)} and Cl_{C4(anti)}). In this case the ΔH[‡] is negative by 3 kcal/mol with respect to the separated reactants, and only 2 kcal/mol higher than the van der Waals complexes. The ΔH_r is lower than that of the *syn*



conformer ($\Delta H_r = -38$ kcal/mol) due to the fact that the reactants are higher in energy, and that the ring closure of $CI_{C2(anti)}$ and $CI_{C4(anti)}$ yield the RR/SS diastereoisomers which are more stable than the RS/SR ones formed by the ring closure of $CI_{C2(syn)}$ and $CI_{C4(syn)}$. The activation enthalpy calculated for the cycloaddition of $CI_{C9\beta pin}$ in the most stable *syn* conformation is equal to 11.7 kcal/mol, a value significantly larger than that calculated for the CIs discussed above. Correspondingly, the ΔH_r is equal to about -24 kcal/mol, more than 10 kcal/mol higher than that calculated for the other CIs. The reaction of the less stable *anti* conformer has an energy profile similar to that of the *syn* conformer with ΔH^\ddagger and ΔH_r equal to -8 and -26 kcal/mol, respectively. The difference in reactivity of $CI_{C9\beta pin}$ compared to the other CIs may be due to the connectivity of the carbon atom of the carbonyl oxide, which in $CI_{C9\beta pin}$ is bound to two other carbons. It is worth noting that the same trend in activation and reaction energies was observed for the addition of DMPO to the two CIs generated by the ozonolysis of α -pinene that we have previously investigated.¹⁸ The two adducts have one and two alkyl substituents attached to the carbon atom of the carbonyl oxide, and feature energy barriers and reaction energies that differ by more than 10 kcal/mol in favour of the less substituted species. CI_{C3Al} is the species featuring the largest difference in the reactivity of the *syn* and *anti* conformers. Considering the most stable *syn* conformer, it turns out that ΔH^\ddagger and ΔH_r are equal to 8.0 and -25 kcal/mol, which are values similar to those calculated for $CI_{C9\beta pin}$. On the other hand, considering the less stable *anti* conformer, the energy profile is much more favourable as the barrier is equal to about -2 kcal/mol with respect to the separated reactants (+5.2 kcal/mol with respect to the van der Waals complex) and the ΔH_r is equal to -33 kcal/mol, values that fit better those calculated for CI_{C2} and CI_{C4} . Figure 4 summarizes the results presented above showing the reaction energy profiles for the formation of the CI-DMPO adducts starting from the CIs in the more stable (Figure 4a) and less stable (Figure 4b) conformations. These results show that the reaction of the investigated CIs with DMPO occurs very rapidly, with the exception of $CI_{C9\beta pin}$ for which, in both conformations the activation energies are larger than those calculated for the other CIs. In addition, all reactions are strongly exothermic, but with the ΔH_r value that becomes significantly less negative with increasing the number of substituents of the carbonyl oxide carbon atom (i.e. the ΔH_r of the $CI_{C9\beta pin}$ -DMPO adduct is more than 15 kcal/mol higher than that of CI_{C1} -DMPO).



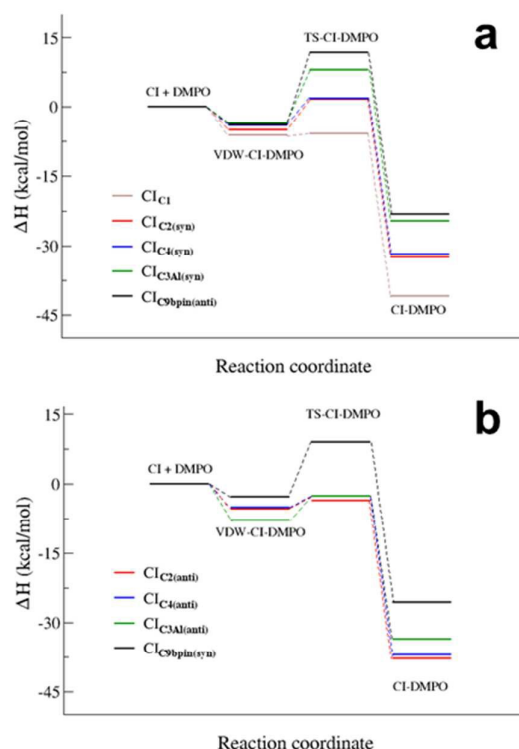


Figure 4. Reaction energy profiles of the CI + DMPO → CI-DMPO reactions of CI_{C1}, CI_{C2}, CI_{C4}, CI_{C9βpin} and CI_{C3Al} calculated starting from the more stable (a) and the less stable (b) conformation of each adduct.

It also worth noting that for all CIs investigated the less stable conformer has a more favourable energy profile. In particular, CI_{C3Al}, which is characterized by the larger difference in stability of the conformers, also features the larger change in the reactivity of such conformers. A similar behaviour has been observed experimentally by Taatjes et al.⁸ who reported that *anti* (less stable) conformer of acetaldehyde oxides is more reactive than the *syn* one with both H₂O and SO₂.

3.2. Detection of CIs in the gas phase from biogenic and anthropogenic VOCs

The adduct formed between the spin trap DMPO and the β-pinene CIs, with the elemental formulas C₁₅H₂₆NO₃⁺ (*m/z*=268.1907) and C₇H₁₄NO₃⁺ (*m/z*=160.0968), were detected by the PTR-ToF-MS (Figure 5a) using the optimised conditions described above. This is consistent with previous studies using IR detection of CIs¹⁴ and our previous work on α-pinene¹⁸ in which the CI-DMPO with elemental formula C₁₆H₂₈NO₄⁺, was detected at *m/z* 298.2013 (the two expected α-pinene CIs are indistinguishable in MS as the double bond is in endo position and the two CIs have the same mass). The reaction mechanism of the formation of the CI-DMPO adduct was elucidated in our previous study¹⁸ and theoretical calculations were used to assess CI-specific stability of the spin trap adducts (Section 3.1).

The observed concentrations of the two CI-DMPO adducts are about three to four orders of magnitude lower compared with the initial concentration of the reagents, which were 18, 83 and 110 ppm for O₃, β-pinene and DMPO respectively. The concentrations of CI-DMPO adducts are also about three and four orders of magnitude lower compared with the steady-state concentration of β-pinene (Table 2) which is in excess with respect to ozone. Notably, ozone can react not only with alkenes but also with the spin trap DMPO, therefore decreasing its concentration and decreasing the efficiency of the spin trapping reaction. For this reason, in the series of experiments we report here, ozone concentration was lower than in the previous experiments performed with α-pinene¹⁸ and in most of the cases was the limiting reagent, in order to minimise losses of DMPO (see VOC concentrations in Table 2).



The concentrations of the CI-DMPO adducts obtained are stable over time scales of one hour or more in the steady-state flow tube set up used here (Figure 5 and Figure 6) and well reproducible in this system, with a variation of $\pm 25\%$ on average observed in multiple repeats. The slow initial increase in CI-DMPO concentration is likely associated with a varying amount of O_3 produced from the UV lamp. In fact, the UV lamp has a warm up time of about 20-30 minutes in which ozone concentration exponentially increases before reaching a plateau (Figure S2). After the UV lamp is switched off, the concentration of CI-DMPO adducts decreases slowly to zero, probably due to memory effects as the DMPO and its adducts can condense on the walls of the tubings.

Similarly, for cis-2-hexene the two expected CI-DMPO adducts with molecular formulas $C_{10}H_{20}NO_3^+$ and $C_8H_{16}NO_3^+$ have been detected at m/z 202.1438 and 174.1125 respectively and, likewise, they are stable over time in the steady-state reaction system (Figure 5b). Additional experiments in which both β -pinene and cis-2-hexene have been concurrently injected in the flow tube have been carried out. Also in this case, all four expected CIs from both VOCs have been detected with good repeatability as shown in Figure 5c. To the authors' knowledge, this is the first time in which detection and identification of CIs from multiple VOC precursors is achieved, clearly demonstrating the capability of this technique to characterise CIs in complex, atmospherically relevant VOC mixtures. Concentrations of CIs from cis-2-hexene are higher than the concentrations of CIs from β -pinene (Table 2) which is consistent with the higher initial concentration of cis-2-hexene (153 ppm) than that of β -pinene (96 ppm).

Furthermore, the study has been additionally extended to other VOCs with different chemical properties and volatilities. Methacrolein, a first-generation oxidation product from isoprene, has been ozonolysed in the flow tube and the two expected CIs have been detected, the CI_{C1} -DMPO and the aldehydic CI_{C3Al} -DMPO (Figure 6a). Also for styrene, an aromatic olefin, both the CI_{C1} -DMPO and the aromatic CI_{C7Ar} -DMPO have been detected (Figure 6b).

Concerning limonene, a diene monoterpene, all CIs from the reaction of ozone with both the endo- and exo- double bond have been detected (Figure 6c). From the comparison between the rate of the reaction of ozone with limonene and that of ozone with limononaldehyde, and the low yields of limona ketone, the ozonolysis of limonene should occur predominantly at the endo-double bond (95:5).³⁸ However, ozone was in excess in our conditions (18 ppm of ozone and 6 ppm of limonene) which can explain the high concentration of CIs detected from the less favoured reaction channel. No second generation CIs were detected from reaction of ozone with an olefinic first-generation oxidation product, but these CIs are likely to be very low-volatility compounds and they probably partition quickly into the condensed phase.

In general, detected mixing ratios of CIs are between three and five orders of magnitude lower than the initial concentrations of the olefinic precursor and between two to four orders of magnitude lower than the measured concentration of olefinic precursor at the steady state (see Table 2). The concentration of olefinic precursors is generally in excess with respect to ozone, except for limonene. During the three seconds reaction time in the flow tube, CIs can decompose to form a wide range of further products, including dioxiranes and vinylhydroperoxides which retain the same molecular mass as the CIs. According to the reaction mechanism proposed by Adam et al.³⁹ the reaction of dioxirane with DMPO yields a product with a mass different to the CI-DMPO adducts. As pointed out by Liu et al.⁴⁰ the vinylhydroperoxide forms with a significant excess energy and rapidly undergoes O–O bond fission to form $\cdot OH$. Nevertheless, the presence of organic acids may help to dissipate the excess energy and stabilise this species so it has to be assessed in future studies whether the vinylhydroperoxide may interfere to some degree with the measurement.

Because of the high VOC concentrations used here, their instrumental signals are likely outside of the linear range of the instrument and therefore the steady-state concentrations derived may be lower limits of their actual concentrations in the flow tube. Other factors should be optimised and characterised for an improved quantification of the CI-adducts, including the effect of secondary organic aerosol formation in the flow tube, wall losses throughout the system, the unknown kinetics



of the CI-spin trap reactions, and unknown fragmentation patterns of the CI-DMPO adducts in the mass spectrometer. To the authors' knowledge, this is the first time in which detection of CIs from methacrolein, limonene, styrene and cis-2-hexene is achieved, and the first time in which four CIs from a mixture of two olefinic precursors were simultaneously detected.

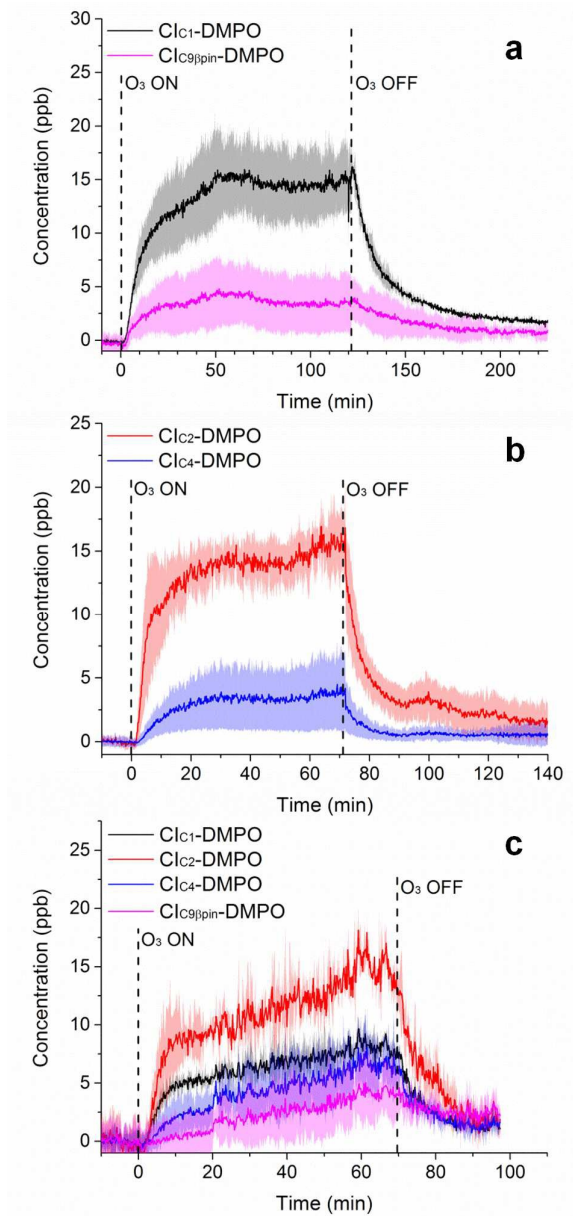


Figure 5. Time-series of CIs formed from the ozonolysis of β -pinene (a), cis-2-hexene (b) and a mixture of β -pinene and cis-2-hexene (c) in a steady-state flow tube reaction system.

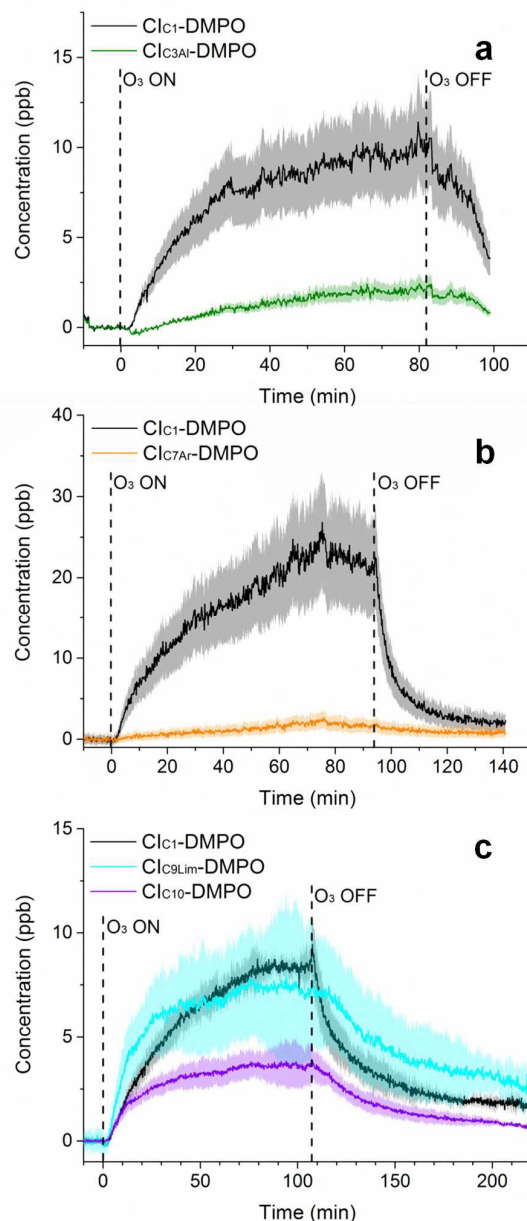


Figure 6. Time-series of CIs formed from the ozonolysis of methacrolein (a), styrene (b) and limonene (c) in a steady-state flow tube reaction system. For limonene ozonolysis, the Cl_{C10Al} and Cl_{C10K} have the same exact mass, therefore are indistinguishable in MS and reported here as one time trace (Cl_{C10}).

3.3. Comparison between experimental measurements and MCM modelling

To compare our experimental results and test the quantification capability of the technique in our experimental conditions, experimental results have been compared with MCM model simulations. The complexity of the entire ozonolysis reaction scheme is vast, and a plethora of compounds produced in this system can scavenge CIs, including the carbonyl compound produced in a 1:1 ratio during the first steps of the reaction. Whilst not a fully explicit chemical mechanism, the MCM can help in understanding the complexity of the system and evaluate the amount of both excited and stabilised CIs available at the outlet of the flow tube (3 seconds reaction time) in the experiments performed.



The results of the AtChem/MCM modelling simulating the experiment of ozonolysis of the VOC mixture containing β -pinene and cis-2-hexene are reported in Figure 7. The results show the decay of β -pinene, cis-2-hexene and ozone with a time resolution of one second (Figure 7a) in which it can be seen that after a three seconds reaction time in the flow tube, concentrations of β -pinene and cis-2-hexene are still very high as ozone is not in excess and its concentration in turns rapidly decreases. It can also be seen in Figure 7c that excited CIs decompose quickly in the flow tube and their concentrations in our steady-state reaction system is lower than the detection limits (~ 30 ppt)¹⁸. Conversely, detectable amounts in the ppb range of SCIs are still present at the end of the flow tube (Figure 7d) and can therefore be detected by our technique.

The results of the AtChem/MCM modelling for all other VOCs are reported in Figure S3 to S7, showing the time-series of VOCs and ozone consumption, and excited and stabilised CIs production. In general, the results of the AtChem/MCM model show that the ozonolysis reaction is very fast in our experimental conditions and the excited CIs decompose quickly in the flow tube so that their concentrations (mostly below ppb levels) are estimated to be far below detection limits at the mixing point with DMPO (after 3 seconds reaction time) for all experiments. On the contrary, detectable amounts in the ppb range of SCIs are still present at the end of the flow tube and they can therefore be trapped by the DMPO. Our results show that the method used here it is suitable for detection of SCIs in laboratory experiments. Further studies are needed to investigate the possibility of detecting excited CIs.

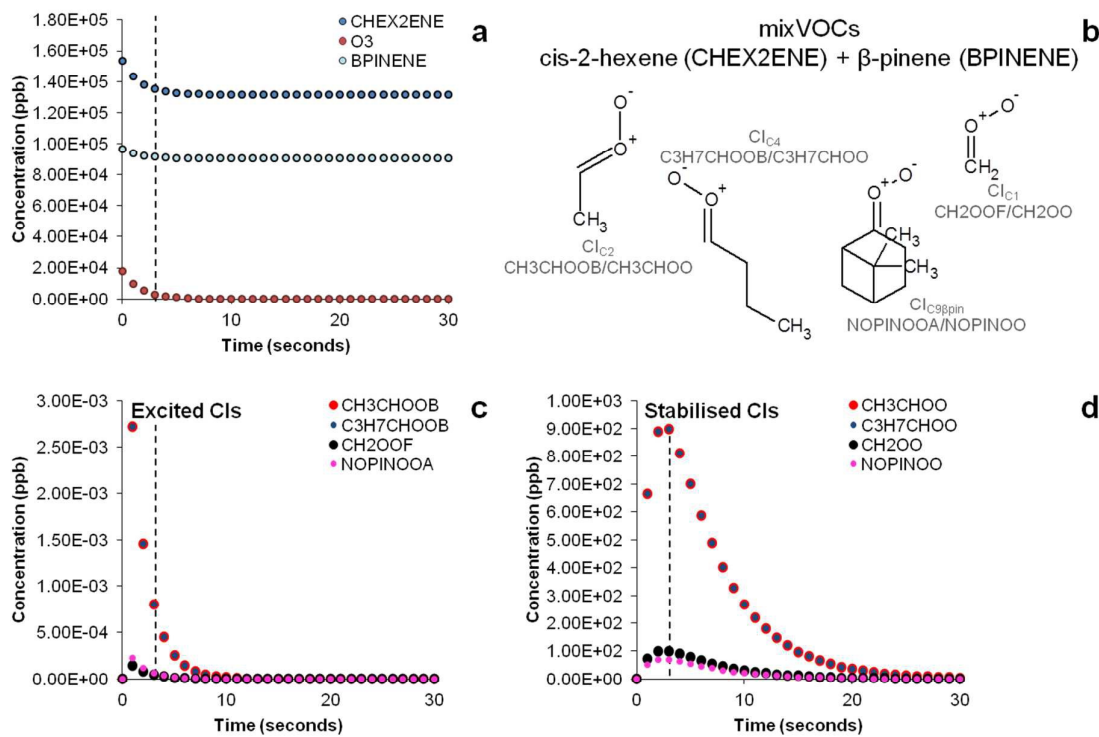


Figure 7. Time evolution of precursors (a), structures and acronyms of CIs (b) and time evolution of excited CIs (c) and stabilised CIs (d) in the ozonolysis of a VOC mixture of β -pinene and cis-2-hexene determined by the MCM model simulating our experimental conditions. Dashed vertical bars indicate reaction time (3 seconds) in our steady-state flow tube experiments during which ozone reacts with the olefinic precursors producing CIs before they are mixed with the DMPO.

The comparison between theoretically expected concentration of SCIs and experimental measurements of CI-DMPO adducts is reported in Table 2. Results show that measured concentrations of CI-DMPO adducts are at least one order of magnitude lower than the modelled concentrations of SCIs from the AtChem/MCM model. This may be explained with wall losses in the systems, which were not estimated. Efficiency of the spin trapping reaction should be good as ozone was generally the limiting reagent, to minimise reaction with DMPO, and DMPO was at least 4 orders of magnitude in excess with respect to the CIs. Nevertheless, reaction kinetics of SCIs with DMPO are unknown and this could also partly explain the discrepancy between experimental measurements and modelling results. The discrepancy is larger for the $\text{CI}_{\text{C9}\beta\text{pin}}$ for which the reaction with DMPO has a larger energy barrier decreasing the adduct formation rate (Figure 6). In addition, the fragmentation pattern of CIs-DMPO adducts in the PTR-ToF-MS is unknown which can lead to an underestimation of CIs-DMPO concentration. Nevertheless, MCM is not a fully explicit mechanism and, for example, does not include self-reaction of SCIs, overestimating SCI concentrations.⁴¹

The measured ratios of CIs produced from the different precursors do not match well the theoretically calculated distribution from the AtChem/MCM model. For example, for the ozonolysis of β -pinene, the MCM model predicts a distribution of 59% of SCI_{C1} and 41% of $\text{SCI}_{\text{C9}\beta\text{pin}}$ while the experimentally measured distribution is 80% of CI_{C1} -DMPO and 20% of $\text{CI}_{\text{C9}\beta\text{pin}}$ -DMPO. This large discrepancy can be explained by considering the stability of the CI-DMPO adducts. The results of the DFT calculations show that the CI_{C1} -DMPO is more stable than the $\text{CI}_{\text{C9}\beta\text{pin}}$ -DMPO. In addition, larger CIs, like $\text{CI}_{\text{C9}\beta\text{pin}}$ and CI_{C7Ar} , were generally measured at lower concentrations than expected from the modelling which might be because of the low volatility of these large CIs resulting potentially in wall losses. However, the temperature of the line after the DMPO mixing point was kept at 85°C to minimise condensation on the walls. Volatility-related artefacts could help explaining why there is a better match between measurements and modelling results for smaller CIs compared to the large β -pinene $\text{CI}_{\text{C9}\beta\text{pin}}$ and styrene CI_{C7Ar} .

In future studies, experimental strategies to improve quantification could aim to account for both stability of the CI-DMPO adducts, as adducts with lower stability tends to be more underestimated, and their volatility because some of the adducts have rather high molecular weights, and partitioning into the condensed phase may be non-negligible. This seems to be suggested also by the memory effects in the system (i.e., the slow decrease of signal after the production of ozone in the flow tube is turned off, Figure 5 and Figure 6).

In the case of limonene, the MCM reaction scheme considers only the addition of ozone to the double bond in endo position as the endo-double bond is more reactive than the exo-double bond (95:5).³⁸ However, in our experiments, all CIs from the reaction of ozone with both the endo- and exo-double bond have been detected, with ozone being in excess compared with limonene. However, surprisingly the CI-DMPO from the reaction of ozone with the exo-double bond were detected at higher concentrations than the CI-DMPO from reaction at the endo-double bond. This may be explained by different stabilities and volatilities of the CI-DMPO adducts.

Second generation CIs from the ozonolysis of the olefinic oxidation products from limonene were not detected in this series of experiments which is consistent with theoretical calculations (Figure S8), which predict concentrations in the orders of magnitude below detection limits. However, second generation CIs may be produced in the condensed phase as the oxidation products from limonene ozonolysis are likely to partition efficiently into the particle phase.

Simulations of the AtChem/MCM model in which ozone concentration was changed according to the output of the UV lamp (Figure S2) show that the initial increase of the concentrations of CIs-DMPO adducts before reaching a plateau it is mainly due to the warming up time of the UV lamp before it reaches a constant ozone output (Figure 8).



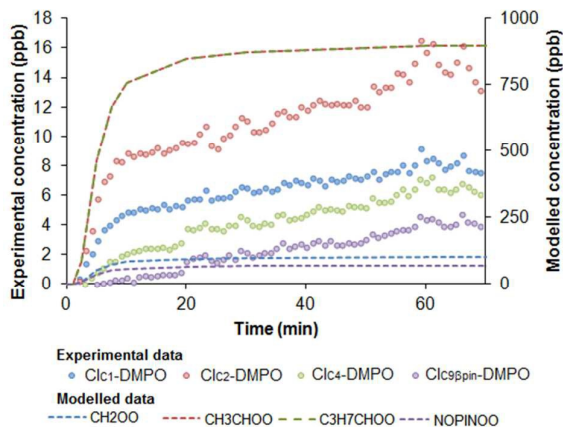


Figure 8. Time evolution of Cls-DMPO adducts (experimental) and SCIs (modelled) in the ozonolysis of a VOC mixture of β -pinene and cis-2-hexene. AtChem/MCM model simulation was run at different initial concentrations of ozone to simulate the warming-up time of the UV lamp used to generate ozone.

Table 2. Initial and steady-state concentrations of VOCs in our experiments and comparison between experimental measurement and expected concentration of Cls from MCM modelling for all VOCs examined in this study and the VOC mixture.

VOCs	Measured [VOC] ₀ (ppm) ^a	Measured [VOC] _{ss} (ppm) ^b	Cl _s -DMPO	Measured [Cl _s - DMPO] _{ss} (ppb) ^c	Measured ratios [Cl _s - DMPO]:[V OC] ₀	Measured fraction (%) of Cl _s - DMPO ^c	Modelle d [SCIs] (ppb)	Modelled fraction (%) of SCIs
β-pinene	83	65±2	Cl _{C1} -DMPO	14.8±3.6	2·10 ⁻⁰⁴	79.6±33.5	250	59.1
			Cl _{C9βpin} -DMPO	3.8±2.8	5·10 ⁻⁰⁵	20.4±16.6	173	40.9
cis-2-hexene	120	24±1	Cl _{C2} -DMPO	14.5±1.9	1·10 ⁻⁰⁴	80.6±22.7	875	50
			Cl _{C4} -DMPO	3.5±2.6	3·10 ⁻⁰⁵	19.4±15.2	875	50
mixVOCs:								
β-pinene	96	55±13	Cl _{C1} -DMPO	6.8±1.1	7·10 ⁻⁰⁵	24.3±7.8	101	5.1
			Cl _{C9βpin} -DMPO	2.6±2.4	3·10 ⁻⁰⁵	9.3±9.0	69	3.5
cis-2-hexene	153	88±6	Cl _{C2} -DMPO	11.8±1.6	8·10 ⁻⁰⁵	42.1±13.1	897	45.7
			Cl _{C4} -DMPO	4.9±2.2	3·10 ⁻⁰⁵	17.5±9.3	897	45.7
methacrolein	838	369±419	Cl _{C1} -DMPO	8.7±1.3	1·10 ⁻⁰⁵	84.5±19.4	334	93.8
			Cl _{C3Al} -DMPO	1.6±0.5	2·10 ⁻⁰⁶	15.5±5.6	22	6.2
limonene	6.3	1.4±0.3	Cl _{C1} -DMPO	7.8±0.6	1·10 ⁻⁰³	42.2±10.1	0.5	0.3
			Cl _{C9Lim} -DMPO	7.2±2.8	1·10 ⁻⁰³	38.9±17.5	0	0
			Cl _{C10K/C10Al} -DMPO	3.5±0.8	6·10 ⁻⁰⁴	18.9±6.1	169 ^d	99.7
styrene	78	8±3	Cl _{C1} -DMPO	18.6±5.2	2·10 ⁻⁰⁴	93.5±38.4	191	50
			Cl _{C7Ar} -DMPO	1.3±0.8	2·10 ⁻⁰⁵	6.5±4.5	191	50

^a Concentration measured in dilution experiments. ^b Experimental uncertainty expressed as standard deviation between 2-3 repeated experiments. Larger uncertainties affect the most volatile VOCs for difficulties in maintaining a constant gas phase concentration in our experimental set-up. ^c Experimental uncertainty expressed as standard deviation between 2-3 repeated experiments. It does not take into account systematic errors due to unknown fragmentation pattern. ^d Referred to SCI_{C10K}.

4. Conclusions

We identified and estimated concentrations of a series of SCIs from the ozonolysis of both biogenic and anthropogenic VOCs by using stabilisation with the spin trap DMPO and analysis with PTR-

ToF-MS. This method proved to be applicable to SCIs with a wide range of structures and allowed us to measure SCIs that were otherwise out of reach for techniques used in previous studies. In addition, for the first time, it was possible to study an even more complex reaction system consisting of more than one olefinic precursor with the simultaneous detection of four SCIs. The method has great potential to be used for quantification of SCIs in laboratory experiments although specific calibration procedures need to be developed to improve accuracy, including assessment of instrumental response at high VOC concentration and estimating fragmentation patterns of CI-DMPO adducts and reaction kinetics between CIs and spin traps. The integrated approach used in this study combining DFT calculations to determine the stability of the CI-DMPO adducts, experimental measurements and MCM modelling revealed the importance of assessing the stability of the adducts to aid interpretation of measurement results but also volatility in the case of larger SCIs. In this context, synthesis of more volatile nitron spin traps may help to overcome this weakness. The suitability of the technique to characterise excited CIs will need to be determined in future studies.

According to recent estimates, ambient SCI concentration in Hyytiälä (Finland) in the summer of 2010 was about 5×10^4 molecules cm^{-3} with an order of magnitude uncertainty.¹⁶ Such concentration levels are about four to five orders of magnitude lower than the detection limits of our instrument¹⁸ and extremely challenging for any instrumental technique currently available even with an *ad hoc* pre-concentration method. Nevertheless, our new technique is uniquely capable of quantifying many different SCIs simultaneously and thus provides a significant step towards studying SCIs in realistic, complex reaction mixtures in the laboratory.

The method proposed here can be used for direct kinetic measurements however the reactivity of the spin trap toward ozone represents a limiting factor on the range of reaction conditions that can be tested. Generation of CIs in ozone-free conditions, e.g. via diiodoalkane photolysis method,⁶ would allow to perform kinetic experiments and compare our method with other measurement methods like PIMS and IR/UV spectroscopy.

Recently, extremely low-volatile organic compounds (ELVOC) have been discovered, which irreversibly condense into the particle phase enhancing, and in some cases dominating, the early stage of atmospheric aerosol formation (nucleation), constituting a crucial link between new particle formation and cloud condensation nuclei formation.^{42,43} The suggested formation pathway of ELVOC from biogenic VOCs relies on initiation via ozonolysis of terpenes, and therefore CI formation, followed by an autoxidation process involving molecular oxygen (vinylhydroperoxide pathway).^{42,44} Measurement of terpenes derived CIs using spin traps as CI scavengers may help in mechanistic studies to elucidate ELVOC formation mechanism, and their role in particle nucleation.

Acknowledgements

This work was funded by the European Research Council (ERC starting grant 279405) and NERC (NE/K008218/1). ATA thanks NERC for funding through NCAS.

References

- 1 J. Clayden, N. Greeves, S. Warren and P. Wothers, *Organic Chemistry (1st ed.)*, Oxford University Press, 2001.
- 2 O. Horie and G. K. Moortgat, *Acc. Chem. Res.*, 1998, **31**, 387–396.
- 3 D. L. Osborn and C. A. Taatjes, *Int. Rev. Phys. Chem.*, 2015, **34**, 309–360.
- 4 R. Criegee, *Angew. Chemie Int. Ed. English*, 1975, **14**, 745–752.
- 5 D. Johnson and G. Marston, *Chem. Soc. Rev.*, 2008, **37**, 699.
- 6 O. Welz, J. D. Savee, D. L. Osborn, S. S. Vasu, C. J. Percival, D. E. Shallcross and C. A. Taatjes, *Science (80-.)*, 2012, **335**, 204–7.
- 7 D. Stone, M. Blitz, L. Daubney, N. U. M. Howes and P. Seakins, *Phys. Chem. Chem. Phys.*,



- 2014, **16**, 1139–49.
- 8 C. A. Taatjes, O. Welz, A. J. Eskola, J. D. Savee, A. M. Scheer, D. E. Shallcross, B. Rotavera, E. P. F. Lee, J. M. Dyke, D. K. W. Mok, D. L. Osborn and C. J. Percival, *Science*, 2013, **340**, 177–80.
- 9 R. Chhantyal-Pun, A. Davey, D. E. Shallcross, C. J. Percival and A. J. Orr-Ewing, *Phys. Chem. Chem. Phys.*, 2014, **17**, 3617–3626.
- 10 W. Chao, J.-T. Hsieh, C.-H. Chang and J. J.-M. Lin, *Science (80-.)*, 2015, **347**, 751–754.
- 11 T. R. Lewis, M. A. Blitz, D. E. Heard and P. W. Seakins, *Phys. Chem. Chem. Phys.*, 2015, **17**, 4859–4863.
- 12 J. M. Beames, F. Liu, L. Lu and M. I. Lester, *J. Am. Chem. Soc.*, 2012, **134**, 20045–8.
- 13 Y.-T. Su, Y.-H. Huang, H. A. Witek and Y.-P. Lee, *Science (80-.)*, 2013, **340**, 174–176.
- 14 J. Ahrens, P. T. M. Carlsson, N. Hertl, M. Olzmann, M. Pfeifle, J. L. Wolf and T. Zeuch, *Angew. Chemie - Int. Ed.*, 2014, **53**, 715–719.
- 15 R. L. Mauldin, T. Berndt, M. Sipilä, P. Paasonen, T. Petäjä, S. Kim, T. Kurtén, F. Stratmann, V.-M. Kerminen and M. Kulmala, *Nature*, 2012, **488**, 193–6.
- 16 A. Novelli, K. Hens, C. Tatum Ernest, M. Martinez, A. C. Nölscher, V. Sinha, P. Paasonen, T. Petäjä, M. Sipilä, T. Elste, C. Plass-Dülmer, G. J. Phillips, D. Kubistin, J. Williams, L. Vereecken, J. Lelieveld and H. Harder, *Atmos. Chem. Phys. Discuss.*, 2016, 1–60.
- 17 O. Horie, C. Schäfer and G. K. Moortgat, *Int. J. Chem. Kinet.*, 1999, **31**, 261–269.
- 18 C. Giorio, S. J. Campbell, M. Bruschi, F. Tampieri, A. Barbon, A. Toffoletti, A. Tapparo, C. Paijens, A. J. Wedlake, P. Grice, D. J. Howe and M. Kalberer, *J. Am. Chem. Soc.*, 2017, submitted.
- 19 J. Zhao and R. Zhang, *Atmos. Environ.*, 2004, **38**, 2177–2185.
- 20 L. Cappellin, M. Probst, J. Limtrakul, F. Biasioli, E. Schuhfried, C. Soukoulis, T. D. Märk and F. Gasperi, *Int. J. Mass Spectrom.*, 2010, **295**, 43–48.
- 21 T. Su, *J. Chem. Phys.*, 1994, **100**, 4703–4703.
- 22 R. Ahlrichs, M. Bar, M. Haser, H. Horn, C. Kolmel, M. Bär, M. Häser, H. Horn and C. Kölmel, *Chem. Phys. Lett.*, 1989, **162**, 165–169.
- 23 A. D. Becke, *Phys. Rev. A*, 1988, **38**, 3098–3100.
- 24 J. P. Perdew, *Phys. Rev. B*, 1986, **33**, 8822–8824.
- 25 A. D. Becke, *J. Chem. Phys.*, 1993, **98**, 5648–5652.
- 26 C. Lee, W. Yang and R. Parr, *Phys. Rev. B*, 1988, **37**, 785–789.
- 27 P. Stephens, F. Devlin, C. Chabalowski and M. Frisch, *J. Phys. Chem.*, 1994, **98**, 11623–11627.
- 28 K. Eichkorn, F. Weigend, O. Treutler and R. Ahlrichs, *Theor. Chem. Acc.*, 1997, **97**, 119–124.
- 29 A. Schäfer, C. Huber and R. Ahlrichs, *J. Chem. Phys.*, 1994, **100**, 5829.
- 30 S. F. Boys and F. Bernardi, *Mol. Phys.*, 1970, **19**, 553–566.
- 31 F. Furche and R. Ahlrichs, *J. Chem. Phys.*, 2002, **117**, 7433–7447.
- 32 H. Weiss, R. Ahlrichs and M. Häser, *J. Chem. Phys.*, 1993, **99**, 1262–1270.
- 33 M. E. Jenkin, S. M. Saunders, V. Wagner and M. J. Pilling, *Atmos. Chem. Phys.*, 2003, **3**, 181–193.
- 34 M. J. Newland, A. R. Rickard, M. S. Alam, L. Vereecken, A. Muñoz, M. Ródenas and W. J. Bloss, *Phys. Chem. Chem. Phys.*, 2015, **17**, 4076–4088.
- 35 R. Gutbrod, E. Kraka, R. N. Schindler and D. Cremer, *J. Am. Chem. Soc.*, 1997, **119**, 7330–7342.
- 36 J. M. Anglada, J. M. Bofill, S. Olivella and A. Solé, *J. Am. Chem. Soc.*, 1996, **118**, 4636–4647.
- 37 L. Vereecken and J. S. Francisco, *Chem. Soc. Rev.*, 2012, **41**, 6259.
- 38 IUPAC, *IUPAC Task Group on Atmospheric Chemical Kinetic Data Evaluation – Data Sheet Ox_VOC20*, 2013.



- 595 39 W. Adam, K. Briviba, F. Duschek, D. Golsch, W. Kiefer and H. Sies, *J. Chem. Soc. Chem.*
596 *Commun.*, 1995, 1831–1832.
- 597 40 F. Liu, Y. Fang, M. Kumar, W. H. Thompson and M. I. Lester, *Phys. Chem. Chem. Phys.*,
598 2015, **17**, 20490–20494.
- 599 41 Y.-T. Su, H.-Y. Lin, R. Putikam, H. Matsui, M. C. Lin and Y.-P. Lee, *Nat. Chem.*, 2014, **6**,
600 477–83.
- 601 42 M. Ehn, J. A. Thornton, E. Kleist, M. Sipilä, H. Junninen, I. Pullinen, M. Springer, F.
602 Rubach, R. Tillmann, B. Lee, F. Lopez-Hilfiker, S. Andres, I.-H. Acir, M. Rissanen, T.
603 Jokinen, S. Schobesberger, J. Kangasluoma, J. Kontkanen, T. Nieminen, T. Kurtén, L. B.
604 Nielsen, S. Jørgensen, H. G. Kjaergaard, M. Canagaratna, M. Dal Maso, T. Berndt, T. Petäjä,
605 A. Wahner, V.-M. Kerminen, M. Kulmala, D. R. Worsnop, J. Wildt and T. F. Mentel,
606 *Nature*, 2014, **506**, 476–9.
- 607 43 J. Tröstl, W. K. Chuang, H. Gordon, M. Heinritzi, C. Yan, U. Molteni, L. Ahlm, C. Frege, F.
608 Bianchi, R. Wagner, M. Simon, K. Lehtipalo, C. Williamson, J. S. Craven, J. Duplissy, A.
609 Adamov, J. Almeida, A.-K. Bernhammer, M. Breitenlechner, S. Brilke, A. Dias, S. Ehrhart,
610 R. C. Flagan, A. Franchin, C. Fuchs, R. Guida, M. Gysel, A. Hansel, C. R. Hoyle, T. Jokinen,
611 H. Junninen, J. Kangasluoma, H. Keskinen, J. Kim, M. Krapf, A. Kürten, A. Laaksonen, M.
612 Lawler, M. Leiminger, S. Mathot, O. Möhler, T. Nieminen, A. Onnela, T. Petäjä, F. M. Piel,
613 P. Miettinen, M. P. Rissanen, L. Rondo, N. Sarnela, S. Schobesberger, K. Sengupta, M.
614 Sipilä, J. N. Smith, G. Steiner, A. Tomè, A. Virtanen, A. C. Wagner, E. Weingartner, D.
615 Wimmer, P. M. Winkler, P. Ye, K. S. Carslaw, J. Curtius, J. Dommen, J. Kirkby, M.
616 Kulmala, I. Riipinen, D. R. Worsnop, N. M. Donahue and U. Baltensperger, *Nature*, 2016,
617 **533**, 527–531.
- 618 44 T. F. Mentel, M. Springer, M. Ehn, E. Kleist, I. Pullinen, T. Kurtén, M. Rissanen, A. Wahner
619 and J. Wildt, *Atmos. Chem. Phys.*, 2015, **15**, 6745–6765.
- 620
621

